J. Plant Biol. (2014) 57:291-301
DOI 10.1007/s12374-014-0041-1

ORIGINAL ARTICLE

Roles of the Nuclear-Encoded Chloroplast SMR Domain-Containing PPR Protein SVR7 in Photosynthesis and Oxidative Stress Tolerance in *Arabidopsis*

He-Xin Lv[1,2], Chao Huang[3], Guang-Qin Guo[2] and Zhong-Nan Yang[3,*]

[1]*School of Biotechnology, Tianjin University of Science & Technology, Tianjin 300457, China*
[2]*Institute of Cell Biology, School of Life Sciences, Lanzhou University, 222 South Tianshui Road, Lanzhou 730000, China*
[3]*College of Life and Environmental Sciences, Shanghai Normal University, 100 Guilin Road, Shanghai 200234, China*

Received: January 22, 2014 / Accepted: July 26, 2014

Abstract The mutations of the plastid SMR domain-containing PPR protein SVR7 were previously reported to cause a specific reduction in the chloroplast ATP synthase levels. Here, we isolated a new mutant allele of *SVR7*, named *svr7-4*, in which T-DNA is inserted into the initiation codon of *SVR7*. The rosette leaves of *svr7-4*, especially in the juvenile stage, showed a pale green phenotype as a result of a reduction in the chlorophyll levels. The values of P700 and Fv/Fm indicated that the photosynthetic capacities of both PSI and PSII were damaged in *svr7-4*. Furthermore, we found that the *svr7-4* accumulated more reactive oxygen species (ROS) and showed lower photo-oxidative stress tolerance by histochemical staining and hydrogen peroxide bleaching experiments, respectively. The leaves of *svr7-4* also had increased anthocyanins accumulation compared to that of wild-type (WT) when floated on water under light. Finally, we found that the expression levels of four abiotic stress-responsive genes including *ZAT10*, *AtAPX1*, *CAT1* and *AtGPX2* were up-regulated in *svr7-4*. *SVR7* was expressed ubiquitously during plant development. These results indicate that *SVR7* is important for normal photosynthesis and photo-oxidative stress responses in chloroplasts.

Keywords: Chloroplast, Oxidative stress, Pentatricopeptide repeat domain, Photosynthesis, Reactive oxygen species, Small mutS-related domain

*Corresponding author; Zhong-Nan Yang
Tel : +86-21-64324190
E-mail : znyang@shnu.edu.cn

Introduction

Chloroplasts are essential organelles that are found in plant cells and eukaryotic algae. In addition to conducting photosynthesis, chloroplasts perform other essential processes including the biosynthesis of amino acids, lipids, fatty acids, hormones, nucleotides, vitamins and secondary metabolites (Leister, 2003). The origin of chloroplasts can be traced to an endosymbiotic event in which a free-living cyanobacterium-like prokaryote invaded a eukaryotic cell, followed by the large-scale genes being gradually transferred to the host nucleus (Timmis et al. 2004). Altogether, a functional chloroplast contains approximately 3,000 proteins, although only approximately 100 proteins are products of the chloroplast genome; the remaining proteins are transcribed in the nucleus and then imported into the chloroplast after being translated in the cytosol (Martin and Herrmann 1998; Leister 2003). Therefore, the biogenesis and functions of chloroplasts are highly dependent on nuclear genes.

Nuclear-encoded chloroplast-targeted protein factors are involved in overall chloroplast functions, such as photosynthesis, plastid metabolism, chloroplast and host cell biogenesis, or in nuclear-chloroplast trafficking and signaling (Næsted et al. 2004). Pentatricopeptide repeat (PPR) proteins are defined by a signature motif (PPR motif) of a degenerate 35-amino-acid repeat that is often arranged in tandem arrays of 2-27 repeats per peptide (Lurin et al. 2004). The PPR protein family contains many members (~450 members in Arabidopsis thaliana) (Schmitz-Linneweber and Small 2008). Many PPR proteins are localized in chloroplasts and are involved in RNA cleavage, RNA editing, RNA splicing, RNA stability, and the translation of their target transcripts (Kotera et al. 2005; Schmitz-Linneweber et al. 2006; Falcon de Longevialle et al. 2007, 2008; Okuda et al. 2007, 2009; Chateigner-

Boutin et al. 2008; Beick et al. 2008; Tavares-Carreón et al. 2008; Yu et al. 2009; Zhou et al. 2009). This family has been divided into two subfamilies, the P subfamily with members that are composed only of PPR motifs and the PLS subfamily (Aubourg et al. 2000; Lurin et al. 2004). The PLS subfamily has been further subdivided into four subgroups including PLS, E, E+ and DYW, according to the variable tandem repeat non-PPR motifs at the C-terminus (Lurin et al. 2004).

P subfamily PPR proteins can also be categorized by the presence of additional domains, such as the small MutS-related (SMR) domain (Delannoy et al. 2007). The SMR domain was originally identified in the C-terminal region of the bacterial MutS2 protein from the cyanobacterium *Synechocystis* (Moreira and Philippe, 1999). Bacterial SMR domains can bind branched DNA structures such as Holliday junctions, D-loops, and pseudo-Y structures (Pinto et al. 2005; Kang et al. 2005; Fukui et al. 2008). SMR domains have endonuclease activity and act in DNA recombination and repair processes (see a review in Fukui and Kuramitsu, 2011). In Arabidopsis, there are eight SMR domain-containing PPR proteins. Three of these proteins have experimental data. *Genomes uncoupled 1* (*GUN1*) is the key component in the plastid-to-nucleus retrograde signaling pathways that couple photosynthesis-related nuclear gene expression and chloroplast functions (Koussevitzky et al. 2007; Cottage et al. 2010). pTAC2 is a member of the transcriptionally active chromosome and is essential for the transcription of the plastid-encoded RNA polymerase (PEP)-dependent plastid genes (Pfalz et al. 2006). Recently, the third PPR-SMR protein SUPPRESSOR OF VARIEGATION 7 (SVR7) was analyzed (Liu et al. 2010). The *svr7* mutant was identified during a screen for suppressors of the *var2* phenotype. The Arabidopsis *var2* mutant displays a unique green and white/yellow leaf variegation phenotype and lacks VAR2, a plastid-localized homolog of the FtsH class of ATP-dependent metalloproteases (Chen et al. 2000; Takechi et al. 2000). The *SVR7* mutation suppresses the variegated phenotype of *var2* by an unknown mechanism (Liu et al. 2010). Zoschke et al. (2013) demonstrated that the *SVR7* mutation impairs the accumulation and translation of chloroplast ATP synthase subunits. In addition, a reduced ribosome association of *atpB/*

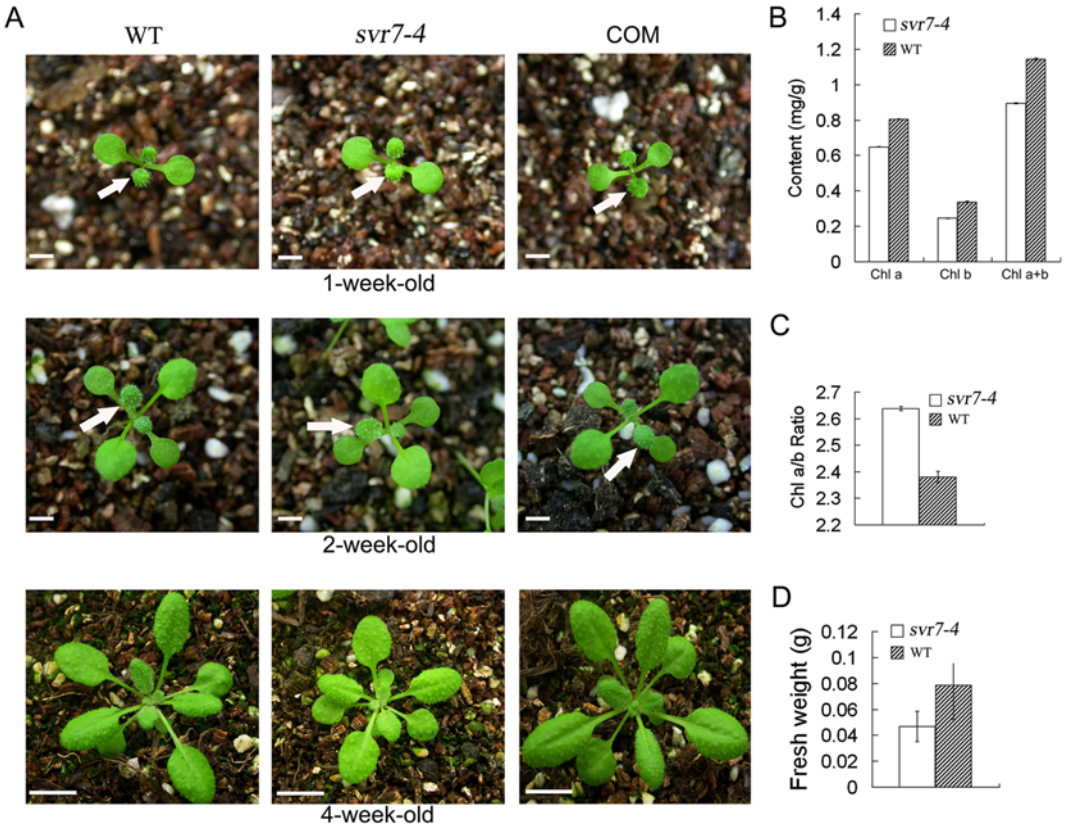

Fig. 1. Phenotypic analysis of the *var7* mutant and WT. (A) One-, two- and four-week-old plants grown in the growth chamber. The arrows indicate the different pale green phenotypes between the *svr7-4* mutants and wild-type. WT, wild-type. COM, genetic complementation line. Bars = 0.2 cm in one and two-week-old plants. Bars = 1 cm in four-week-old plants. (B) Leaf comparisons of chlorophyll a, b and total content of four-week-old *svr7-4* mutant and WT. Values shown are averages ±SD of three replicated experiments. (C) Comparison of chlorophyll a/b ratio of four-week-old *svr7-4* mutant and WT. Values shown are averages ±SD of three replicated experiments. (D) Comparison of fresh weight between four-week-old *svr7-4* mutant and WT. Values shown are averages ±SD of a population of 40 plants.

E and *rbcL* mRNAs in the *svr7* mutants suggests the involvement of SVR7 in the translational activation of these mRNAs (Zoschke et al. 2013).

In this study, we have analyzed a mutant allele of *SVR7*. *svr7-4* exhibits a pale green phenotype and decreased photosynthetic capacity. The *svr7-4* also exhibits enhanced sensitivity to oxidative stress and increased accumulation levels of reactive oxygen species (ROS). Further investigation found that the expression of some antioxidative genes that are involved in responding to ROS was up-regulated in *svr7-4*, which may help scavenge the excess accumulation of ROS. These results indicate that *SVR7* is important for normal photosynthesis and the chloroplast response to photo-oxidative stress.

Results

Phenotypic and Genetic Analysis of the *svr7-4* Mutant

When identifying new genes that are essential for chloroplast development and photosynthesis, we identified a T-DNA insertion line in Arabidopsis ecotype Col-0 with pale green rosette leaves and a relatively dwarf phenotype (Fig. 1A). The total chlorophyll content was slightly reduced in the mutant (Fig. 1B). However, the chlorophyll a/b ratio of the mutant increased by 9.6% compared to that of the WT (Fig. 1C). In addition, we quantitatively evaluated the smaller stature of the mutant plants by measuring the fresh weight of four-week-old whole plants. Results showed that the fresh weight of the mutant plants decreased by 40% compared to that of the WT plants that were grown under the same conditions (Fig. 1D). When the mutant was crossed with the WT, the F1 plants exhibited a normal phenotype. The segregation ratio between the green and pale green plants in the F2 population was close to 3:1 (green:pale green = 61:20, $\chi^2 = 0.012$, $P > 0.95$). These results demonstrate that the mutant phenotype is the result of a single, recessive, nuclear mutation.

We used thermal asymmetric interlaced PCR (TAIL-PCR) to identify the T-DNA insertion site in this mutant. Sequencing of the TAIL-PCR products revealed that the T-DNA was

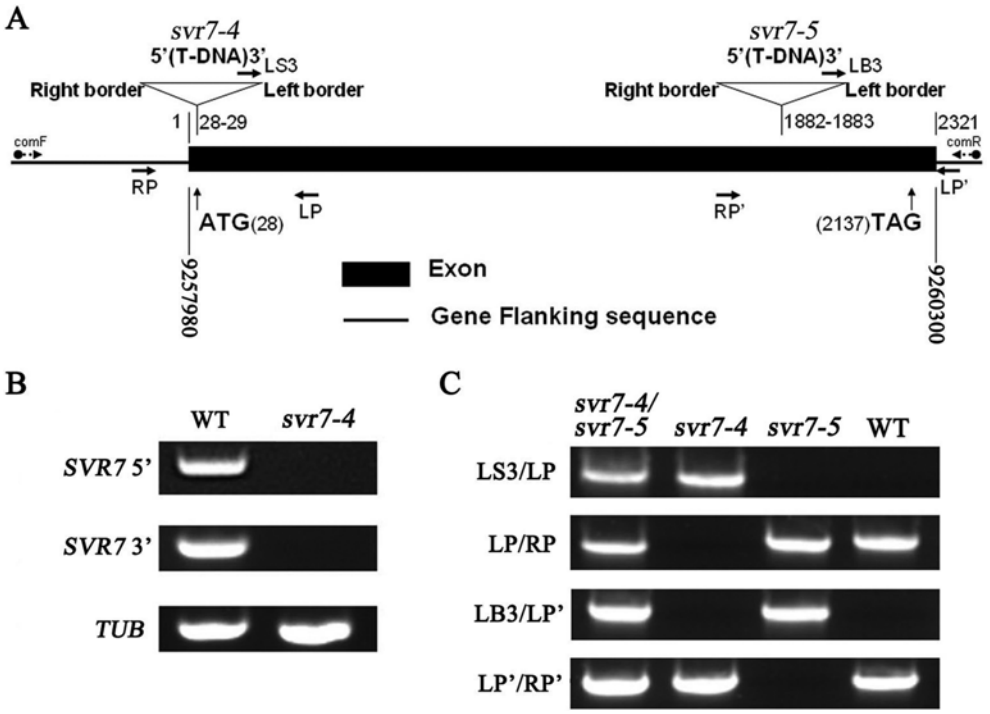

Fig. 2. Indentification and characterization of the *SVR7* gene. (A) Schematic diagram of the *SVR7* gene. Exon (black box) and gene flanking sequence (line) are indicated. The positions of the T-DNA insertions corresponding to *svr7-4* and SAIL3_42_G09 (*svr7-5*) mutants are shown. LS3/LB3, T-DNA specific primer set; LP/RP and LP'/RP' primer sets, used for T-DNA insertion validation in *svr7-4* and *svr7-5* mutants are shown (arrows). comF/comR primer set (dashed arrows) used for genetic complementation is shown. The upright numbers are used to indicate *SVR7* nucleotide position on chromosome IV. The horizontal numbers are used to indicate the nucleotide positions on the *SVR7* transcript. (B) Expression analysis of *SVR7* and the neighboring gene in the WT and mutant. *SVR7 5'* indicates the genomic region expression by the primer set that flank the T-DNA insertion in the *svr7-4* mutant; *SVR7 3'* indicates the genomic region expression by the primer set located at the 3' region not flanking the T-DNA insertion in the *svr7-4* mutant; *TUBULIN* (*TUB*) expression was used as the control. (C) PCR analysis of the allele tests. *svr7-4/ svr7-5* was used to indicate the F1 progeny of two alleles. LS3/LP, LB3/LP' were used to validate the existence of the T-DNA insertion. LP/RP, LP'/RP' were used to validate the F1 progeny genotypes. *svr7-4, svr7-5* and WT were used as controls.

inserted at a position between the A and T of the initiation codon of the gene *AT4G16390* (*SVR7*) in the Arabidopsis genome (Fig. 2A). Reverse transcription (RT)-PCR demonstrated that the *SVR7* transcripts cannot be detected in the mutant (Fig. 2B). To confirm that the knockout of SVR7 was responsible for the defects in this mutant, a construct containing the genomic sequence of the *AT4G16390*, as well as a 1766-bp upstream sequence and 164-bp downstream sequence were introduced into the heterozygous plant (Fig. 2A). Two of three transgenic plants were completely rescued (Fig. 1A). This mutant was named *svr7-4* because three mutant alleles of *SVR7* had been previously described (Liu et al. 2010;

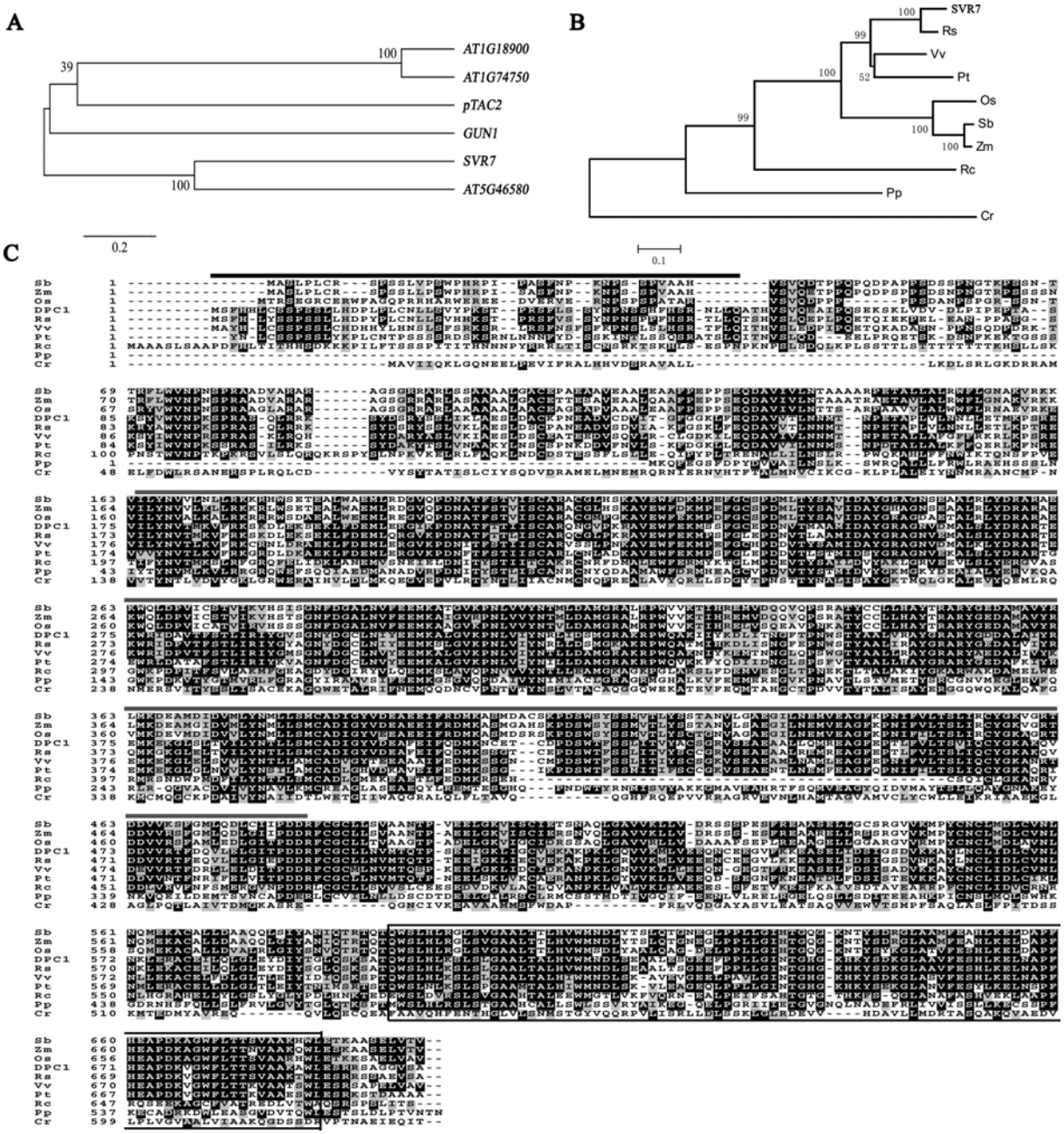

Fig. 3. Phylogenetic analysis of SVR7 homologues. (A) Unrooted phylogenetic tree of six *Arabidopsis* PPR and SMR domain containing proteins. (B) Unrooted phylogenetic tree of the SVR7 and its homologues from various species. Rs, *Raphanus sativus*, P67.1; Vv, *Vitis vinifera*, CAO43700; Os, *Oryza sativa*, Os03g0215900; Pp, *Physcomitrella patens* subsp. XP_001779433; Cr, Chlamydomonas *reinhardtii*, XM_001691012; Pt, *Populus trichocarpa*, AC216943; Sb, *Sorghum bicolor*, XP_002465641; Zm, *Zea mays*, NP_001130387; Rc, *Ricinus communis*, EEF42446. (C) Multiple alignments of SVR7 and homologues. Black bars, predicted transit peptide sequence of SVR7; Gray bars, PPR domain of SVR7; Box, SMR domain of SVR7. Sequences were aligned using CLUSTAL X (2.0) (Thompson *et al*., 1997) and displayed using BOXSHADE (www.ch.embnet.org/software/BOX_form.html).

Zoschke et al. 2013). In addition, we obtained one individual *svr7* allele from the Syngenta Arabidopsis Insertion Library (SAIL) collection at the Arabidopsis Biological Resource Center (ABRC), *svr7-5* (SAIL_423_G09) (Fig. 2A, C), which exhibited the same phenotype as that of *svr7-4* (data not shown). The results of the allele test by crossing the two alleles (*svr7-4* and *svr7-5*) demonstrated that the *AT4G16390* knockout resulted in the pale-green and dwarf phenotype of the *svr7* mutant.

The Phylogenetic Analysis of the SVR7 Sequence

In the Arabidopsis genome, there are eight proteins with PPR and SMR domains. A phylogenetic analysis conducted by MEGA 4.1 (Tamura et al. 2007) grouped SVR7 and an unknown gene (*AT5G46580*) into the same clade with a 34.5% sequence identity (Fig. 3A). The *SVR7* and *AT5G46580* expression patterns were also similar based on microarray data in the Genevestigator V3 analysis tool (https://www.genevestigator.ethz.ch/) (Zimmermann et al. 2004; Grennan, 2006) and the gene co-expression database (http://www.arabidopsis.leeds.ac.uk/act/) (Manfield et al. 2006). The second gene of close homology to SVR7 was GUN1 (Fig. 3A), which shares approximately 19.6% protein sequence homology with SVR7. GUN1 is a component of retrograde signal transduction localized in chloroplasts (Koussevitzky et al. 2007). To investigate whether the chloroplast-to-nucleus retrograde signaling process of *svr7* is abrogated or impaired as in the *gun1* mutant, the expression of *Lhcb1.2* was investigated under photo-oxidative conditions in the presence of 5 μM norflurazon. Real-time RT-PCR demonstrated that *Lhcb1.2* expression was down-regulated in both *svr7* and WT plants at the seedling stage, indicating that the chloroplast-to-nucleus retrograde signaling process was not affected in the *svr7* mutant (data not shown). Another member of this phylogenetic tree, pTAC2 (Pfalz et al. 2006), is a component of the plastid genome transcription active site (Koussevitzky et al. 2007). These results suggest that SVR7 might also play an important role in the chloroplast.

A PSI-BLAST search identified homologs of the SVR7 protein in various plant species including rice, radish, grape, moss, cottonwood, castor, maize, sorghum and chlorophytes (http://www.ncbi.nlm.nih.gov/). The PPR and SMR domain homologs were aligned by CLUSTAL X (2.0) (Thompson et al. 1997), and a phylogenetic tree was constructed using MEGA 4.1 (Tamura et al. 2007) (Fig. 3B, C). The radish protein P67, which has been reported as a chloroplast RNA-binding protein (Lahmy et al. 2000), had an 86.3% amino

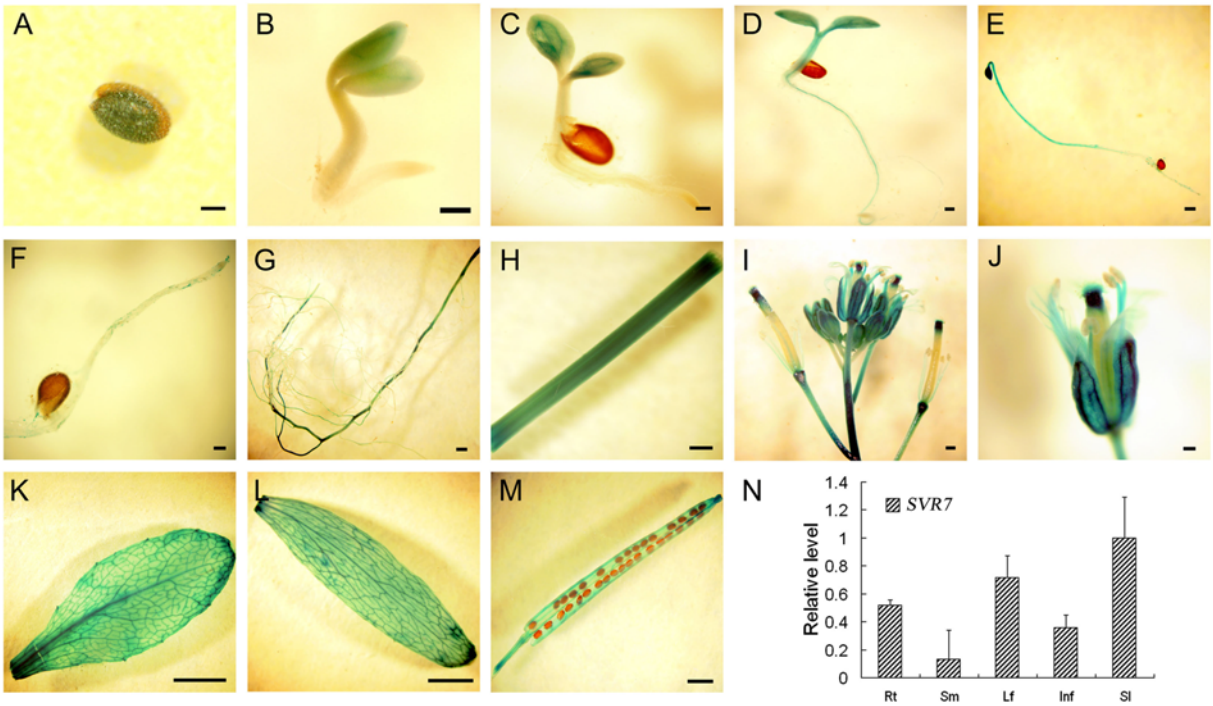

Fig. 4. *SVR7* expression pattern. *SVR7*-driven GUS expression assay. (A) Histochemical staining of globular embryo in seeds imbibed in water for 2 d at 4°C. (B-D) one-, two- and three-d-old seedlings. (E, F) three-d-old seedlings. (G) roots; (H) stems; (I, J) inflorescence and flowers; (K, L) rosettes and cauline leaves; (M) siliques. Bar = 100 μm in (A), bar = 200 μm in (B), bar = 250 μm in (C), bar = 350 μm in (D), bar = 300 μm in (E) and (F), bar = 400 μm in (G, H, I, J and M), bar = 500 μm in (K, L). (N) *SVR7* mRNA abundance in different tissues and growth stages. Rt, root; Sm, stem; Lf, leaf; Inf, inflorescence; Sl, seedling. Values shown are averages ± SD of three replicates of Real-time RT-PCR experiments.

acid sequence identity with SVR7.

SVR7 Expression Pattern

To determine the temporal and spatial expression patterns of *SVR7*, a vector with a 1778-bp upstream genomic fragment of *SVR7* and the coding sequence of the β-glucuronidase (GUS) reporter gene was constructed and introduced into WT. Histochemical staining of the transgenic lines revealed that the *SVR7* gene was expressed in seeds that were imbibed in water for 2-d at 4°C (Fig. 4A), but not in dry seeds (data not shown). In one- and two-d-old germinated seedlings, GUS activity was detected in the cotyledons but not in the hypocotyls (Fig. 4B, C). GUS activity was also detected in every tissue of three-d-old seedlings (Fig. 4D). In the roots, the GUS activity was mainly confined to the primary roots and was weak in the lateral roots (Fig. 4G). GUS staining was also observed in the sepals, petals, stigmas and filaments of the inflorescence but not in the ovaries and stamens (Fig. 4I, J). The GUS expression patterns suggest that *SVR7* is expressed during every stage of the life cycle in different organs (Fig. 4A-M). We also used real-time RT-PCR to further analyze the expression of *SVR7* in different plant organs (roots, stems, leaves, inflorescence and seedlings) from 40-d-old reproductive growth-stage plants and 7-d-old seedlings. Results showed that *SVR7* was highly expressed in the seedlings, leaves and roots; expressed at moderate levels in the inflorescence; and expressed at lower levels in the stems (Fig. 4N), which was consistent with the above GUS staining results. These results indicate that *SVR7* is expressed ubiquitously during plant development.

In addition, we also investigated the effect of light on *SVR7* gene expression. The 3-d-old dark grown seedlings exhibited GUS activity similar to their light-grown counterparts (Fig. 4E, F), indicating that *SVR7* expression is independent of light regulation. Light is one of the most important signals influencing chloroplast development. Light triggers the differentiation of nonphotosynthetic proplastids into fully functional photosynthetic chloroplasts (Lopez-Juez and Pyke, 2005). The light-independent expression of *SVR7* suggests that *SVR7* might play basic roles not only in chloroplast development but also in other types of plastids, which is consistent with the observation that *SVR7* is also expressed in non-green organs, such as roots and petals.

The Reduced Photosynthetic Capacity of *svr7-4*

Leaf coloration mutants are usually tightly linked with abnormal chloroplast development. To understand the physiological role of SVR7 in chloroplast development, we used light micrographs and transmission electron microscopy (TEM) to examine the chloroplast ultrastructure of the *svr7-4* and WT

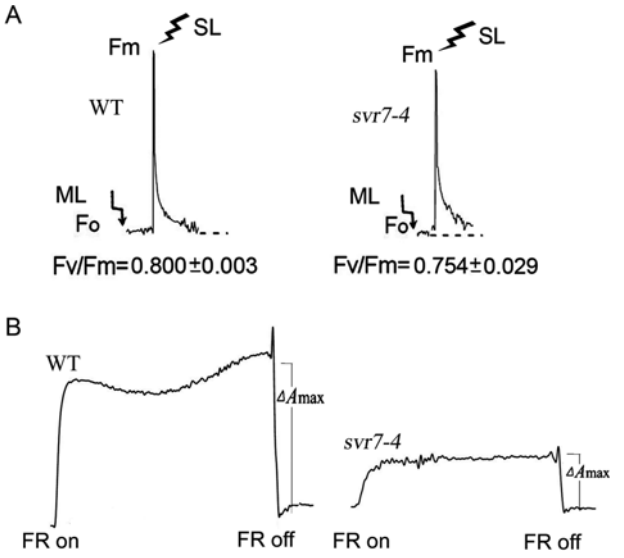

Fig. 5. Spectroscopic analysis of *svr7-4* and WT. (A) Comparison of leaf Fv/Fm ratio between 15 min dark-adapted four-week-old *svr7-4* mutant and WT. The minimal level of fluorescence (F_o) from dark-adapted whole plants with all PSII reaction centers open was determined using a pulsed measuring beam of red light. The Fm level with all PSII reaction centers closed was determined using a saturating pulse and dark-adapted leaves. SL, saturating light; ML, measuring light. Values shown are averages ±SD of three replicated experiments. (B) Redox kinetics of P700. The oxidation of P700 was investigated by measuring absorbance changes of P700 at 820 nm induced by far-red light (FR; 720 nm). *A*max, maximum oxidation induced by far-red light. AL, actinic light.

plants. We found no visible differences in the chloroplast ultrastructure between *svr7-4* and WT (data not shown). In addition, we characterized the photosynthetic capacity of the *svr7-4* mutant. Chlorophyll fluorescence induction experiments demonstrated that the ratio of variable fluorescence to maximum fluorescence (Fv/Fm), which reflects the maximum photochemical efficiency of photosystem II (PSII) was slightly lower in *svr7-4* (0.754±0.029) than that in WT (0.800±0.003) (Fig. 5A). To determine whether the electron transport rate (ETR) of PSI was also blocked in *svr7-4*, we determined the P700 redox kinetics in four-week-old leaves of *svr7-4* and WT under far-red light. As shown in Fig. 5B, a transient increase in the ETR was observed in both the WT and *svr7-4* following the far-red treatment. However, the maximum ETR in *svr7-4* was significantly lower than that in WT (Fig. 5B), indicating that the PSI activity in this mutant was impaired. Taken together, these results indicate that loss of SVR7 affects the PSI more than PSII.

Loss of SVR7 Leads to Increased Sensitivity to Oxidative Stress

Oxidative injury is believed to cause a number of defects in

plants. We analyzed the H_2O_2 and O_2^- accumulation in *svr7-4* through DAB- and NBT-staining, respectively. Histochemical analyses indicated that the *svr7-4* leaves accumulated higher levels of H_2O_2 and O_2^- than that of the WT leaves (Fig. 6A), suggesting that *SVR7* plays an important role in controlling ROS production. To verify this result, *svr7-4* and WT leaves were floated on different concentrations of H_2O_2 and exposed to 120 μmol m^{-2} s^{-1} light for 12 h. The *svr7-4* leaves were bleached in 1.5 M H_2O_2, while the WT leaves showed slower bleaching phenomenon compared to the *svr7-4* mutant under the same condition (Fig. 6B). However, the leaves that were grown under dark conditions showed no obvious differences between *svr7-4* and WT (Fig. 6B). These results indicate that the capacity to detoxify H_2O_2 was obviously decreased in the *svr7-4* mutant. Anthocyanins in vegetative tissues have been proposed to absorb excess light energy to prevent photoinhibition (Smillie and Hetherington 1999; Merzlyak and Chivkunova 2000; Feild et al. 2001). The *svr7-4* leaves accumulated more anthocyanins than that in the WT when floated on water under 120 ìmol m^{-2} s^{-1} light for 60 h (Fig. 6C). The ZAT10/12 transcriptional factors play key roles in modulating plant defense responses (Mittler 2002; Davletova et al. 2005). Some antioxidant genes, such as *AtAPX1*, *CAT1* and *AtGPX2*, are induced by ROS (Mylona and Polidoros 2010). Therefore, we detected the expression levels of these genes in *svr7*. The real-time PCR results indicate that the transcriptional levels of *ZAT10*, *AtAPX1*, *CAT1* and *AtGPX2* were significantly up-regulated in *svr7-4* compared to those of WT. The expression of *ZAT12* was not obviously difference between *svr7-4* and WT (Fig. 6D). These results suggest that *SVR7* may play a role in protecting the chloroplast against oxidative stress.

Discussion

The functions of SVR7 and its orthologous protein P67 in radish and ATP4 in maize have been studied. P67 has RNA-binding activity in vitro (Lahmy et al. 2000). The *atp4* mutant exhibited a pale green phenotype and seedling lethality. Loss of ATP4 function reduced the translation of *atpB/E* and *atpA*, which further affect the chloroplast ATP synthase (Zoschke et al. 2012). Similar to its homologous protein in Arabidopsis, the SVR7 mutation also resulted in the impaired accumulation and translation of chloroplast ATP synthase subunits and reduced ribosome association of *atpB/E* and *rbcL* mRNAs (Zoschke et al. 2013). The reduced accumulation of ATP synthase was considered to affect chloroplast rRNA processing and chloroplast protein accumulation (Liu et al. 2010). In this study, we isolated an allele of *SVR7* that exhibited a reduced growth rate with pale green rosette leaves. The loss of *SVR7* resulted in slightly decreased chlorophyll a and b contents. However, the chlorophyll a/b ratio increased in this mutant, suggesting that the maintenance of chlorophyll-a-rich reaction centers at the expense of chlorophyll-b-rich antenna complexes. Aronsson et al. (2008) suggested that this mechanism enables a more efficient use of light energy with limited pigment resources. Thus, an increase in the chlorophyll a/b radio suggests that *svr7-4* adjusted the two pigment quantities to minimize the damage due to the decreased photosynthetic efficiency.

Plant cells suffer from oxidative stress, of which ROS are the major factors (Zhao et al. 2005). Chloroplasts are the primary source of ROS. The photosynthetic electron transport system generates ROS even under optimal conditions (Asada 1999; Asada 2000). The production of ROS is low in normal plant cells because of well-developed defense systems against ROS (Myouga et al. 2008). Superoxide dismutases (SODs) constitute the first line of cellular defense against ROS, which scavenge the primary product of oxygen reduction, superoxide anion (O_2^-) (Bowler et al. 1994). These superoxide dismutases rapidly convert O_2^- and water to hydrogen peroxide (H_2O_2) and molecular oxygen (O_2) (Asada, 2006), thereby protecting the plant against oxidative damage. A high concentration of ROS causes progressive oxidative damages to lipids, proteins, and DNA, ultimately leading to cell death (Sedelnikova et al. 2010; Adibhatla et al. 2010; Bochkov et al. 2010; Sharma et al. 2012). In this study, we found that the intracellular levels of ROS were increased in the *svr7-4* mutant and that the *svr7-4* mutant exhibited enhanced sensitivity to H_2O_2 (Fig. 6). PSI is mainly located on the surface of the stroma thylakoids and grana thylakoids, and PSII mostly exists within the grana thylakoids. Our results indicated that the mutation in *SVR7* affected PSI more than PSII (Fig. 5), which may be due to the PSI being outside the thylakoids and therefore more easily affected by ROS accumulation in *svr7*. Thus, SVR7 plays a role in protecting chloroplasts from ROS. The increased accumulation of ROS in the *svr7-4* mutant may lead to the decreased photosynthetic efficiency in *svr7-4*, which further affects the growth of this mutant.

Recently, some PPR proteins were reported to be involved in the defense against abiotic stress tolerance (Laluk et al. 2011; Yuan and Liu 2012). PGN is a mitochondrial PPR protein in Arabidopsis that is important for seed germination on NaCl. The loss of PGN function dramatically increased ROS accumulation in seedlings in response to salt stress (Laluk et al. 2011). Yuan et al. (2012) analyzed another mitochondria-targeted PPR protein SLG1 in Arabidopsis. The *slg1* mutant also accumulated more H_2O_2 and grew slowly. In addition, *slg1* exhibited an enhanced response to ABA and increased tolerance to drought stress. The phenotype of *svr7-4* is similar to that of *slg1*. Both of them exhibited relatively dwarf phenotype compared with WT. Thus, PPR

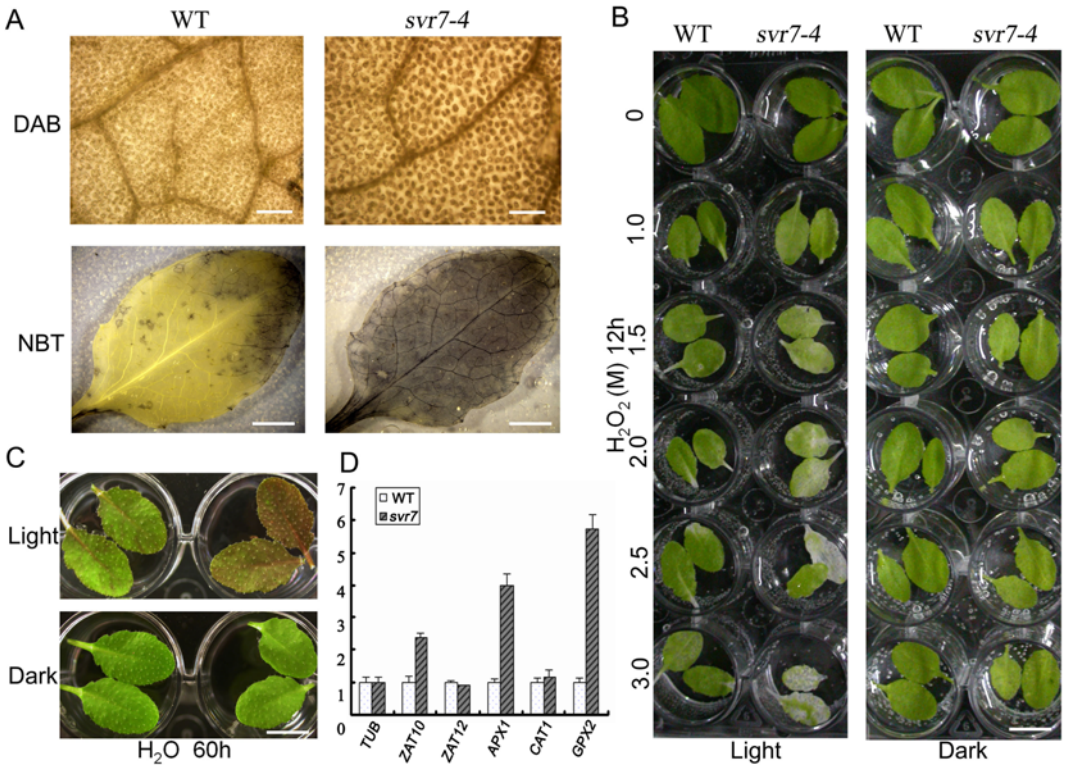

Fig. 6. *svr7-4* accumulates additional ROS. (A) Representative images illustrating H_2O_2 and O_2^- accumulation in the leaves of four-week-old WT and *svr7-4*, visualized by prestaining with 3,3'-diaminobenzidine (DAB, Bars = 25 μm) and nitro blue tetrazolium (NBT, Bars = 30 mm), respectively. (B) Effect of exogenous H_2O_2 on WT and *svr7-4* leaves floated on a H_2O_2 solution at the indicated concentration under 120 μmol m^{-2} s^{-1} light for 12 h. The experiment was repeated more than three times. Bars = 1 cm. (C) Anthocyanin accumulation in leaves floated on water and exposed to 120 μmol m^{-2} s^{-1} light for 60 h. The experiment was repeated more than three times. Bars = 1 cm. (D) Expression analyses of five antioxidant genes in WT and *svr7-4* plants by real-time RT-PCR. mRNA values were normalized against the WT. Values shown are averages ±SD of three replicated experiments.

proteins may play a role in protecting chloroplasts during photosynthesis although their detailed mechanism requires further investigation.

Materials and Methods

Plant Materials and Growth Conditions

The *svr7-4* mutant was isolated from the pSKI015 activation tagging T-DNA mutant pools (Qin et al. 2003). Mutant and WT *Arabidopsis thaliana* plants of the *Columbia*-0 background were chosen for the study. Seeds were sown in pots containing a 6:1:0.5 mix of vermiculite, peat moss and perlite, supplemented with nutrient salts and allowed to imbibe for 3 d at 4ºC. Plants were grown at 22±1ºC in continuous light of 120 μmol m^{-2} s^{-1} or 16-h-light/8-h-dark cycles. Plants were photographed with a Nikon digital camera (COOLPIX 4500; Tokyo, Japan). Transmission electron micrographs were obtained as described by Yu et al. (2009).

Chlorophyll Measurement

Chlorophyll content was determined according to the method described by Lichtenthaler and Wellburn (1983). Total chlorophyll extracts were obtained from 200 mg of fresh leaves from four-week-old mutant and WT plants and subsequently incubated in 10 mL of 80% ethanol under dark until the leaves turned white. Each measurement was performed by three independent repeats and the standard deviations were calculated. Chlorophyll-fluorescence measurements were performed using a pulse amplitude-modulated fluorometer (PAM 101 for P700 measurement and JUNIOR-PAM for Fv/Fm measurement. Heinz Walz GmbH, Effeltrich, Germany) equipped with a data acquisition system to record fast changes (Meurer et al. 1996).

TAIL-PCR and Molecular Cloning of the SVR7 Gene

The presence of the mutant T-DNA insertion was validated by using primers that specifically amplify the T-DNA BAR gene (Bar-F: 5' TCATAGGCGTCTCGCATATCTCA 3'; Bar-R: 5' CTGCACCAT-CGTCAACCACTACA 3'). The tail-PCR procedure with left border primers (LS1, LS2, and LS3) and AD primers followed Liu et al. (1995) and Qin et al. (2003). The T-DNA insertion site and mutant phenotype cosegregation were analyzed with the following LS3 and plant-specific primers (LP: 5'-GGCGCAGTTTCTGGGTTAGT-3'; RP: 5'-TTTGCACGATTCCTTTCATAAC-3'). In the mutant plants, only PCR with LS3 and LP primers amplified a DNA fragment of approximately 700 bp. In the WT, only PCR with LP and RP primers amplified a DNA fragment of 1004 bp. For heterozygous mutant plants, PCR with both primer pairs showed positive results. T-DNA insertion left border specific primer LB3 (5' ATCTGAATTTCAT-AACCAATCTCG 3') and plant-specific LP' (5'TGCCTCATCATCC-GACCA 3') and RP' (5' TGGGAAAGCCAAGCAGGTA 3') were

used in the allele test to identify the *svr7-2* mutant and F1 progeny genotypes. For genetic complementation, a DNA fragment of 4250 bp sequences, including 1792 bp upstream and 348 bp downstream were amplified using Pyrobest-Taq polymerase (Takara, Tokyo, Japan) by the primer set CMF (5' *GAATTC*CCAATAATAGTATTTCGC 3') and CMR (5' *CTGCAG*CAGTTGAAAAACATATC-3'). The *Sma*I and *Sac*I restriction enzyme sites are designated in italics. After sequencing verification, the fragment was cloned into the pCAMBIA1301 binary vector (CAMBIA, ACT, Australia) and introduced into homozygous mutant plants using the infiltration method with *Agrobacterium tumefaciens* strain LBA4404. The transformants were selected on PNS culture medium with 20 mg/L hygromycin and screened for seedlings exhibiting the WT phenotype. As LP/RP-amplified sequences were included in the complementation fragment, for homozygous background verification, the following strategy was adopted: the presence of the T-DNA insertion in the WT hygromycin resistant lines were validated by primer pair LS3 and LP and more than 60 offspring were verified as the presence of the T-DNA insertion in *AT4G16390*.

RNA Extraction and RT-PCR

RNA was prepared as described in Yu et al. (2009). Semi-quantitative RT-PCR was conducted for 35 cycles to assess the *svr7* and WT expression levels using the following primer sets: SVR715'-F (5' AACTGCGAACAAAGTACCCAC 3') and SVR715'-R (5' ATCTT-GCTCAAACAATTTACCAC 3') were used to examine the 5' region expression analysis of *SVR7*; SVR713'-F (5' GTGTACGCTTGT-AGTGGGAGG 3') and SVR713'-R (5' TGTAAGGACCATTGGG-TAGCA 3') were used for the 3' region expression analysis of *SVR7*. 16400RTF (5' TGTCTGGTCGGATGATGAGG 3') and 16400RTR (5' GTGATTGCCATCGCTAAGAA 3') were used for expression analysis of the AT4G16400 gene. β-tubulin (Tub-F: GACACTACA-CTGAAGGTGCTGAG 3' and Tub-R: AAGCTGATGAACAGA-GAGAGTTG) were used as the control. Real-time RT-PCR amplifications were performed with the SYBR GREEN I Kit (TOYOBO, Tokyo, Japan) on an ABI 7300 Real-Time RT-PCR System (Applied Biosystems, MA, USA) and the relative quantification of gene expression data was analyzed as described in Hricová et al. (2006). The primers used to detect expression of the abiotic stress-responsive genes including *ZAT10*, *ZAT12*, *AtAPX1*, *CAT1* and *AtGPX2* were as follows: *ZAT10*F:5'-CCGCCGTGACTACTGGAA-3' and *ZAT10*R: 5'-GATCGGAGGGATGTTGAGG-3', *ZAT12*F: 5'-GTGCGAGTCACAAGAAGCC-3' and *ZAT12*R: 5'-TCGGAAA-CTCCACTCCACAT-3'; *AtAPX1*F: 5'-ACTACCCAACCGTGAG-CGAA-3' and *AtAPX1*R: 5'-TCAAACCTCATTGTTCCGAA-3'; *CAT1*F: 5'-TTACCCAACTTACTTCTGCTG-3' and *CAT1*R: 5'-GATC-AAAGTTCCCCTCTCTG-3'; *AtGPX2*F: 5'-TGGCGGATGAATCT-CCAAAGT-3' and *AtGPX2*R: 5'-GTTCCTTGTAGTTCGCATCCG-3', respectively. The data set was normalized using β-tubulin as the control.

Expression Pattern Analysis

The promoter *SVR7*::GUS was constructed by cloning a 1778-bp upstream genomic sequence before the *SVR7* initiation codon was inserted into the binary vector pCAMBIA1301 of the constitutive CaMV 35S (Cauliflower mosaic virus 35S) promoter prior to GUS removal. The primer set used was as follows: SVR7PF: 5'-*GAATT-C*CCAATAATAGTATTTCGC-3' and SVR7PR: 5'-*GGATCC*TTT-GTTCGCAGTTG-3'. The *Sma*I and *Sac*I restriction enzyme sites are designated in italics. GUS histochemical analysis was performed as described in the Arabidopsis manual (Weigel and Glazebrook 2002). Tissues were examined using a SZ-CTV dissecting microscope interfaced with a DP70 digital camera (Olympus; Tokyo, Japan).

Phylogenetic Analysis

Full-length protein sequence alignment was performed using CLUSTAL X (2.0) (Thompson et al. 1997), and BOXSHADE (http://www.ch.embnet.org/software/BOX_form.html). Phylogenetic trees were constructed by MEGA 4.1 (Tamura et al. 2007).

DAB and NBT Histochemical Staining and Hydrogen Peroxide Bleaching

The leaves of four-week-old mutant and WT plants were vacuum-infiltrated for histochemical detection of H_2O_2 as described by Díaz-Vivancos et al. (2008). Histochemical detection of O_2^- was performed by infiltrating leaves directly with 0.1 mg/mL^{-1} of nitro blue tetrazolium (NBT) (Dingguo, Beijing, China) in 25 mM K-HEPES buffer (pH 7.6) and incubating at 25°C in the dark for 24 h. In both cases, leaves were rinsed in 80% (v/v) ethanol for 10 min at 70°C, mounted in lactic acid:phenol:water (1:1:1, v/v/v), and photographed directly using a SZ-CTV dissecting microscope interfaced with a DP70 digital camera (Olympus, Tokyo, Japan). For hydrogen peroxide bleaching, the leaves of four-week old mutant and WT plants were floated on an H_2O_2 series (0, 1.0, 1.5, 2.0, 2.5, 3.0 M) under 120 μmol m^{-2} s^{-1} light for 12 h; and to assess anthocyanin accumulation, leaves were floated on water under light at 120 μmol m^{-2} s^{-2} for 60 h. Leaves were photographed using a Nikon digital camera (COOLPIX 4500; Tokyo, Japan).

Acknowledgements

This work was supported by the grant of the National Natural Science Foundation of China (31370271).

Author's Contributions

LHX performed chlorophyll measurement, histochemical staining and hydrogen peroxide pleaching experiments; Phylogenetic and expression pattern analysis of SVR7 were performed by HC; LHX and HC wrote the manuscript; GGQ and YZN designed the experimental plan and revised the manuscript. All the authors agreed on the contents of the paper and post no conflicting interest.

References

Adibhatla RM, Hatcher JF (2010) Lipid oxidation and peroxidation in cns health and disease: from molecular mechanisms to therapeutic opportunities. Antioxid Redox Signal 12:125–169

Aronsson H, Schottler MA, Kelly AA, Sundqvist C, Dormann P, Karim S, Jarvis P (2008) Monogalactosyldiacylglycerol deficiency in *Arabidopsis thaliana* affects pigment composition in the prolamellar body and impairs thylakoid membrane energization and photoprotection in leaves. Plant Physiol 148:580–592

Asada K (1999) The water-water cycle in chloroplasts: scavenging of active oxygen and dissipation of excess photons. Annu Rev Plant Physiol Plant Mol Biol 50:601–639

Asada K (2000) The water-water cycle as alternative photon and electron sinks. Philos Trans R Soc Lond B Biol Sci 355:1419–1431

Asada K (2006) Production and scavenging of reactive oxygen species in chloroplasts and their functions. Plant Physiol 141:391–396

Aubourg S, Boudet N, Kreis M, Lecharny A (2000) In *Arabidopsis thaliana*, 1% of the genome codes for a novel protein family unique to plants. Plant Mol Biol 42:603–613

Bochkov VN, Oskolkova OV, Birukov KG, Levonen AL, Binder CJ, Stöckl J (2010) Generation and biological activities of oxidized phospholipids. Antioxid Redox Signal 12:1009–1059

Bowler C, van Camp W, van Montagu M, Inzé D (1994) Superoxide dismutases in plants. Crit Rev Plant Sci 13:199–218

Chateigner-Boutin AL, Ramos-Vega M, Guevara-Garcia A, Andres C, de la Luz Gutierrez-Nava M, Cantero A, Delannoy E, Jimenez LF, Lurin C, Small I, Leon P (2008) CLB19, a pentatricopeptide repeat protein required for editing of *rpoA* and *clpP* chloroplast transcripts. Plant J 56:590–602

Chen M, Choi Y, Voytas DF, Rodermel S (2000) Mutations in the Arabidopsis VAR2 locus cause leaf variegation due to the loss of a chloroplast FtsH protease. Plant J 22:303–313

Cottage A, Mott EK, Kempster JA, Gray JC (2010) The Arabidopsis plastid-signalling mutant *gun1* (*genomes uncoupled1*) shows altered sensitivity to sucrose and abscisic acid and alterations in early seedling development. J Exp Bot 61:3773–3786

Davletova S, Schlauch K, Coutu J, Mittler R (2005) The zinc-finger protein Zat12 plays a central role in reactive oxygen and abiotic stress signaling in Arabidopsis. Plant Physiol 139:847–856

Delannoy E, Stanley WA, Bond CS, Small ID (2007) Pentatricopeptide repeat (PPR) proteins as sequencespecificity factors in post-transcriptional processes in organelles. Biochem Soc Trans 35:1643–1647

Díaz-Vivancos P, Clemente-Moreno MJ, Rubio M, Olmos E, García JA, Martínez-Gómez P, Hernández JA (2008) Alteration in the chloroplastic metabolism leads to ROS accumulation in pea plants in response to plum pox virus. J Exp Bot 59:2147–2160

Fukui K, Kuramitsu S (2011) Structure and function of the small MutS-related domain. Mol Biol Int 2011:691735

Fukui K, Nakagawa N, Kitamura Y, Nishida Y, Masui R, Kuramitsu S (2008) Crystal structure of Muts2 endonuclease domain and the mechanism of homologous recombination suppression. J Biol Chem 283:33417–33427

Hricová A, Quesada V, Micol JL (2006) The SCABRA3 nuclear gene encodes the plastid RpoTp RNA polymerase, which is required for chloroplast biogenesis and mesophyll cell proliferation in Arabidopsis. Plant Physiol 141:942–956

Kang J, Huang S, Blaser MJ (2005) Structural and functional divergence of MutS2 from bacterial MutS1 and eukaryotic MSH4-MSH5 homologst. J Biol Chem 187: 3528–3537

Kotera E, Tasaka M, Shikanai T (2005) A pentatricopeptide repeat protein is essential for RNA editing in chloroplasts. Nature 433:326–330

Koussevitzky S, Nott A, Mockler TC, Hong F, Sachetto-Martins G, Surpin M, Lim J, Mittler R, Chory J (2007) Signals from chloroplasts converge to regulate nuclear gene expression. Science 316:715–719

Lahmy S, Barnèche F, Derancourt J, Filipowicz W, Delseny M, Echeverria M (2000) A chloroplastic RNA-binding protein is a new member of the PPR family. FEBS Letters 480:255–260

Leister D (2003) Chloroplast research in the genomic age. Trends Genet 19:47–56

Lichtenthaler HK, Wellburn AR (1983) Determination of total carotenoids and chlorophylls a and b of leaf extracts in different solvents. Biochem Soc Trans 11:591–592

Liu X, Yu F, Rodermel S (2010) An Arabidopsis pentatricopeptide repeat protein, SUPPRESSOR OF VARIEGATION7, is required for FtsH-mediated chloroplast biogenesis. Plant Physiol 154:1588–1601

Liu YG, Mitsukawa N, Oosumi T, Whittier RF (1995) Efficient isolation and mapping of *Arabidopsis thaliana* T-DNA insert junctions by thermal asymmetric interlaced PCR. Plant J 8:457–463

Lopez-Juez E, Pyke KA (2005) Plastids unleashed: their development and their integration in plant development. Int J Dev Biol 49:557–577

Lurin C, Andrés C, Aubourg S, Bellaoui M, Bitton F, Bruyère C, Caboche M, Debast C, Gualberto J, Hoffmann B, Lecharny A, Le Ret M, Martin-Magniette ML, Mireau H, Peeters N, Renou JP, Szurek B, Taconnat L, Small I (2004) Genome-wide analysis of Arabidopsis pentatricopeptide repeat proteins reveals their essential role in organelle biogenesis. Plant Cell 16:2089–2103

Manfield IW, Jen CH, Pinney JW, Michalopoulos I, Bradford JR, Gilmartin PM, Westhead DR (2006) Arabidopsis Co-expression Tool (ACT): web server tools for microarray-based gene expression analysis. Nucleic Acids Res 34 (Web Server issue):W504–W509

Martin W, Herrmann RG (1998) Gene transfer from organelles to the nucleus: how much, what happens, and why? Plant Physiol 118:9–17

Merzlyak MN, Chivkunova OB (2000) Light-stress-induced pigment changes and evidence for anthocyanin photoprotection in apples. J Photochem Photobiol B 55:155–163

Meurer J, Meierhoff K, Westhoff P (1996) Isolation of high-chlorophyllfluorescence mutants of *Arabidopsis thaliana* and their characterization by spectroscopy, immunoblotting and Northern hybridization. Planta 198:385–396

Mittler R (2002) Oxidative stress, antioxidants and stress tolerance. Trends Plant Sci 7:405–410

Moreira D, Philippe H (1999) Smr: a bacterial and eukaryotic homologue of the C-terminal region of the MutS2 family. Trends Biochem Sci 24:298–300

Mylona PV, Polidoros AN (2010) ROS Regulation of Antioxidant Genes. In: S. Dutta Gupta (ed), Reactive oxygen species and antioxidants in higher plants, Science Publishers, USA, pp:101–127

Myouga F, Hosoda C, Umezawa T, Iizumi H, Kuromori T, Motohashi P, Shono Y, Nagata N, Ikeuchi m, shinozaki k (2008) a heterocomplex of iron superoxide dismutases defends chloroplast nucleoids against oxidative stress and is essential for chloroplast development in Arabidopsis. Plant Cell 20:3148–3162

Næsted H, Holm A, Jenkins T, Nielsen HB, Harris CA, Beale MH, Andersen M, Mant A, Scheller H, Camara B, Mattsson O, Mundy J (2004) Arabidopsis *VARIEGATED 3* encodes a chloroplasttargeted, zinc-finger protein required for chloroplast and palisade cell development. J Cell Sci 117:4807–4818

Okuda K, Myouga F, Motohashi R, Shinozaki K, Shikanai T (2007) Conserved domain structure of pentatricopeptide repeat proteins involved in chloroplast RNA editing. Proc Natl Acad Sci USA 104:8178–8183

Okuda K, Chateigner-Boutin AL, Nakamura T, Delannoy E, Sugita M, Myouga F, Motohashi R, Shinozaki K, Small I, Shikanai T (2009) Pentatricopeptide repeat proteins with the DYW motif have distinct molecular functions in RNA Editing and RNA cleavage in Arabidopsis chloroplasts. Plant Cell 21:146–156

Pfalz J, Liere K, Kandlbinder A, Dietz KJ, Oelmüller R (2006) pTAC2, -6, and -12 are components of the transcriptionally active plastid chromosome that are required for plastid gene expression. Plant Cell 18:176–197

Pinto AV, Mathieu A, Marsin S, Veaute X, Ielpi L, Labigne A, Radicella JP (2005) Suppression of homologous and homeologous recombination by the bacterial MutS2 protein. Mol Cell 17:113–120

Qin G, Kang D, Dong Y, Shen Y, Zhang L, Deng X, Zhang Y, Li S, Chen N, Niu W, Chen C, Liu P, Chen H, Li J, Ren Y, Gu H, Deng XW, Qu LJ, Chen Z (2003) Obtaining and analysis of flanking sequences from T-DNA transformants of Arabidopsis. Plant Sci 165:941–949

Schmitz-Linneweber C, Williams-Carrier RE, Williams-Voelker PM,

Kroeger TS, Vichas A, Barkan A (2006) A pentatricopeptide repeat protein facilitates the trans-splicing of the maize chloroplast rps12 pre-mRNA. Plant Cell 18:2650–2663

Schmitz-Linneweber C, Small I (2008) Pentatricopeptide repeat proteins: a socket set for organelle gene expression. Trends Plant Sci 13:663–670

Sedelnikova OA, Redon CE, Dickey JS, Nakamura AJ, Georgakilas AG., Bonner WM (2010) Role of oxidatively induced DNA lesions in human pathogenesis. Mutat Res 704:152–159

Small ID, Peeters N (2000) The PPR motif-a TPR-related motif prevalent in plant organellar proteins. Trends Biochem Sci 25:46–47

Smillie RM, Hetherington SE (1999) Photoabatement by anthocyanin shields photosynthetic systems from light stress. Photosynthetica 36:451–463

Tamura K, Dudley J, Nei M, Kumar S (2007) MEGA4: Molecular Evolutionary Genetics Analysis (MEGA) software version 4.0. Mol Biol Evol 24:1596–1599

Takechi K, Sodmergen, Murata M, Motoyoshi F, Sakamoto W (2000) The YELLOW VARIEGATED (VAR2) locus encodes a homologue of FtsH, an ATP-dependent protease in Arabidopsis. Plant Cell Physiol 41:1334–1346

Thompson JD, Gibson TJ, Plewniak F, Jeanmougin F, Higgins DG (1997) The ClustalX windows interface: flexible strategies for multiple sequence alignment aided by quality analysis tools. Nucleic Acids Res 25:4876–4882

Timmis JN, Ayliffe MA, Huang CY, Martin W (2004) Endosymbiotic gene transfer: organelle genomes forge eukaryotic chromosomes. Nat Rev Genet 5:123–135

Weigel D, Glazebrook J (2002) Arabidopsis: A Laboratory Manual, Cold Spring Harbor Laboratory Press, New York, pp:243-245

Yu QB, Jiang Y, Chong K, Yang ZN (2009) AtECB2, a pentatricopeptide repeat protein, is required for chloroplast transcript accD RNA editing and early chloroplast biogenesis in *Arabidopsis thaliana.* Plant J 59:1011–1023

Zhao J, Fujita K, Sakai K (2005) Oxidative stress in plant cell culture: a role in production of beta-thujaplicin by *Cupresssus lusitanica* suspension culture. Biotechnol Bioeng 90:621–631

Zhou W, Cheng Y, Yap A, Chateigner-Boutin AL, Delannoy E, Hammani K, Small I, Huang JR (2008) The Arabidopsis gene *YS1* encoding a DYW protein is required for editing of *rpoB* transcripts and the rapid development of chloroplasts during early growth. Plant J 58:82–96

Zoschke R, Kroeger T, Belcher S, Schottler MA, Barkan A, Schmitz-Linneweber C (2012) The pentatricopeptide repeat-SMR protein ATP4 promotes translation of the chloroplast atpB/E mRNA. Plant J 77:547–558

Zoschke R, Qu YJ, Zubo YO, Börner T, Schmitz-Linneweber C (2013) Mutation of the pentatricopeptide repeat-SMR protein SVR7 impairs accumulation and translation of chloroplast ATP synthase subunits in *Arabidopsis thaliana*. J Plant Res 126:403–414